Journal of Pathology
J Pathol 2009; **217**: 524–533
Published online 4 November 2008 in Wiley InterScience
(www.interscience.wiley.com) **DOI:** 10.1002/path.2483

Original Paper

An integrated proteomics approach for studying the molecular pathogenesis of Dupuytren's disease

Sandra Kraljevic Pavelic,[1,2]* Mirela Sedic,[1] Karlo Hock,[1] Srdan Vucinic,[1] Davor Jurisic,[3] Peter Gehrig,[4] Mike Scott,[4] Ralph Schlapbach,[4] Tamara Cacev,[1] Sanja Kapitanovic[1] and Kresimir Pavelic[1,2]*

[1] *Division of Molecular Medicine, Rudjer Boskovic Institute, Bijenicka Cesta 54, 10000 Zagreb, Croatia*
[2] *Department of Biotechnology, University of Rijeka, 51000 Rijeka, Croatia*
[3] *Clinical Hospital Rijeka, Department of Plastic and Reconstructive Surgery, 51000 Rijeka, Croatia*
[4] *Functional Genomics Center Zürich, Winterthurerstrasse 190 (UNI Irchel), CH-8057 Zürich, Switzerland*

**Correspondence to:*
Professor Kresimir Pavelic, MD or Sandra Kraljevic Pavelic, PhD, Rudjer Boskovic Institute, Division of Molecular Medicine, Bijenicka Cesta 54, 10000 Zagreb, Croatia.
E-mail: pavelic@irb.hr, skraljevic@irb.hr

The authors declare that there are no financial/commercial conflicts of interest.

Received: 11 June 2008
Revised: 29 September 2008
Accepted: 20 October 2008

Abstract

Dupuytren's disease (DD) is a fibromatosis characterized by non-malignant transformation of palmar fascia leading to permanent contraction of one or more fingers. Despite the extensive knowledge of its clinical pathogenesis, the aetiology of this disease remains obscure. In the present paper, we report for the first time on the proteomic profiling of diseased versus unaffected patient-matched palmar fasciae tissues from DD patients using two-dimensional gel electrophoresis coupled with mass spectrometry analysis. The herein identified proteins were then used to create the protein–protein interaction network (interactome). Such an integrated approach revealed the involvement of several different molecular processes related to DD progression, including extra- and intra-cellular signalling, oxidative stress, cytoskeletal changes, and alterations in cellular metabolism. In particular, autocrine regulation through ERBB-2 and IGF-1R receptors and the Akt signalling pathway have emerged as novel components of pro-survival signalling in Dupuytren's fibroblasts and thus might provide a basis for a new therapeutic strategy in Dupuytren's disease.

Keywords: Akt; bioinformatics; cytoskeleton; Dupuytren's disease; proteomics

Introduction

Dupuytren's disease (DD) is characterized as a non-malignant transformation of connective tissue beneath the skin of the palm. It affects one or more digits, leading to irreversible contracture and loss of hand function [1]. A characteristic of DD is abnormal proliferation of fibroblasts and their differentiation into myofibroblasts. The latter generate a contractile force as a consequence of smooth muscle α-actin overexpression.

Recent research into fibrotic diseases highlighted the importance of anomalous expression of growth factors, eg tumour growth factors α and β (TGF-α, TGF-β), found to be elevated in DD patients as well [1]. The altered expression of growth factors is accompanied by dense extracellular matrix production [2]. Reactive oxygen species (ROS) may also play a role in DD [3]. Currently, the standard treatment for DD is surgical therapy, which neither cures nor prevents frequent recurrence [2].

In the present study, we performed protein expression profiling of diseased versus unaffected patient-matched palmar fasciae tissues derived from DD patients by means of two-dimensional gel electrophoresis (2-DE) followed by mass spectrometry (MS) identification of the selected protein spots, as described previously [4]. Identified proteins were assigned biological context by creating a protein–protein interactions map (so-called 'interactome'). Such an integrated approach has disclosed possible new players responsible for DD progression.

Materials and methods

Clinical specimens

Tissue samples from 12 patients (male Caucasians of European ethnicity, aged 59–77 years, who underwent partial fasciectomy as treatment of Dupuytren's disease, diagnosed the last residual disease phase) were obtained from the Clinical Hospital 'Dubrava', Zagreb, Croatia. Informed consent was obtained from all patients. The tissues were immediately exhaustively washed in ice-cold isotonic buffer, frozen in liquid nitrogen, and stored at $-80\,^{\circ}C$. Clinical specimens were collected in strict compliance with the clinic's

chief pathologist and the ethics committee for research involving human subjects.

Two-dimensional gel electrophoresis (2-DE)

Diseased and unaffected patient-matched palmar fasciae tissues from 12 Dupuytren's disease patients were divided into two groups (six patient-matched pairs per group), ground under liquid nitrogen, and lysed directly in 1 ml of either CHAPS-based [7 M urea, 2 M thiourea, 4% (w/v) CHAPS, 1% (w/v) DTT] or ASB-14-based [7 M urea, 2 M thiourea, 2% (w/v) ASB-14, 0.5% (w/v) Triton X-100, 1% (w/v) DTT] 2-DE buffer supplemented with 0.2% (w/v) Bio-Lyte ampholyte, pH 3–10 (Bio-Rad, USA), nuclease mix (Amersham BioSciences), and protease inhibitor cocktail (Roche, Switzerland). The insoluble pellet was removed by centrifugation (13 200 rpm, 10 min at 4 °C). Protein quantities were determined by the DC Protein Assay Kit (Bio-Rad, USA). A total of 400 μg of proteins was loaded onto 17 cm IPG strips, pH 3–10 NL (Bio-Rad, USA), and subjected to isoelectric focusing on the Protean IEF cell (Bio-Rad, USA) for approximately 90 000 V h. The proteins were resolved on the vertical 12% polyacrylamide gels by the Protean II XL cell (Bio-Rad, USA). The obtained gels were stained with colloidal Coomassie Blue (Bio-Rad, USA) and scanned by the VersaDoc Imaging System 4000 (Bio-Rad, USA). Image analysis was carried out using PDQuest SW, 7.0 (Bio-Rad, USA), whereby the total density in the gel image was used as a normalization method. The analysis sets were created to compare the gels obtained from patient-matched sample pairs across the same 2-DE buffer type and between the two buffers. The criterion for image analysis was a five-fold change in the spot intensity between diseased and non-diseased samples in all 2-DE gels in the match set [5].

In-gel digestion and mass spectrometry analysis

Differentially expressed protein spots were excised from the gels, digested with trypsin, and spotted on the MALDI plate using a TECAN Genesis ProTeam 150 robot (TECAN AG, Männedorf, Switzerland). Gel plugs were briefly incubated in 50 mM ammonium bicarbonate/30% acetonitrile for 300 s at 37 °C. After buffer removal, wells were heated for 180 s at 60 °C and the plugs incubated in 80% acetonitrile for 600 s. After evaporation, 6.7 ng/μl trypsin in 5 mM Tris, pH 8.3, was added per well followed by incubation for 300 s. Subsequently, 5 μl of 5 mM Tris, pH 8.3, was added and the wells were incubated for 3 h at 37 °C. Upon completion of digestion, 1% TFA was added per well and left for 900 s. Peptides were extracted through previously equilibrated reversed-phase μ-C_{18} ZipTips (Millipore Corporation, Bedford, MA, USA). MALDI matrix solution (4 mg of cyano-4-hydroxycinnamic acid in 65% acetonitrile/35% H_2O containing 0.1% TFA) was aspirated and dispensed through the ZipTip three times to elute peptides onto the MALDI plate.

The samples were analysed on the 4700 Proteomics Analyser MALDI-TOF/TOF system (Applied Biosystems, Framingham, MA, USA) equipped with a Nd : YAG laser operating at 200 Hz. All mass spectra were recorded from 750 to 4000 Da in a positive reflector mode. They were generated by accumulating data from 5000 laser pulses. First, the MS spectra were acquired from the standard peptides on each of the six calibration spots and then the default calibration parameters of the instrument were updated. The MS spectra were recorded for all sample spots on the plate and internally calibrated using signals from autoproteolytic fragments of trypsin. Up to three spectral peaks per spot that met the threshold criterion (S/N > 60) were included in the acquisition list for the MS/MS spectra analysis. Peptide fragmentation was performed at a collision energy of 1 kV and a collision gas pressure of approximately 2×10^{-7} Torr. During MS/MS data acquisition, a minimum of 2500 shots (50 sub-spectra accumulated from 50 laser shots each) and a maximum of 5000 shots (100 sub-spectra) were allowed for each spectrum. The accumulation of additional laser shots was halted whenever at least four ions with a S/N of at least 50 were present in the accumulated MS/MS spectrum in the region from m/z 200 to 90% of the precursor mass.

Protein identification by database searching

GPS (Global Proteome Server) Explorer software version 3.6 (Applied Biosystems) was used for submitting MS and MS/MS data for database searching, and Mascot version 2.1.0 (Matrix Science, London, UK) was utilized as a search engine [6]. Database searching of MS and MS/MS spectra was performed using a human protein sequence database downloaded from the EBI (40 794 sequences; release date: 19 March 2005; source: ftp://ftp.ebi.ac.uk/pub/databases/SPproteomes/fasta/proteomes/25.H_sapiens.fasta.gz). The following search settings were applied: maximum number of missed cleavages: 1; peptide tolerance: 35 ppm; MS/MS tolerance: 0.2 Da. Carboxyamidomethylation of cysteine was set as a fixed modification and oxidation of methionine was selected as a variable modification.

Bioinformatics

The interactome map was constructed from interactions obtained from two free on-line sources: Human Interactome Map (HiMAP [7], http://www.himap.org/) and Search Tool for the Retrieval of Interacting Proteins (STRING [8], http://string.embl.de/). However, it was not possible to design an interactome so as to encompass the entire range of experimentally obtained proteins just by using those proteins alone. Therefore, with the help of these sources, several proteins were added to the experimental set to bring that set together in a single network and complete the map.

Only proteins at most two interaction nodes removed from the empirical set of proteins were used for the interactome (threshold level set at 1X). As a rule, the interactions among these added proteins were not explored in further detail, but rather only their links with the empirically obtained proteins were incorporated in the map design. To facilitate the interpretation of the pictogram, the proteins were categorized by their cellular function and encoded as gene names in the interactome.

Western blot analysis

Tissues were lysed in buffer containing 50 mM HEPES (pH 7.5), 150 mM NaCl, 1 mM EDTA, 0.2 mM EGTA, 10% glycerol, 1% Triton X-100, and protease inhibitor cocktail (Roche, Switzerland). A total of 45 μg of proteins per run were resolved on 9% or 12% SDS-polyacrylamide gels at 100 V and transferred to nitrocellulose membrane at 200 mA using the Mini-PROTEAN Cell (Bio-Rad, USA). Membranes were blocked with 4% non-fat dry milk in TBST (50 mM Tris base, 150 mM NaCl, 0.1% Tween 20, pH 7.5). The membranes were incubated with primary antibodies raised against Akt1/2/3 (Santa Cruz Biotechnology, USA; diluted 1 : 200), p-Akt (New England Biolabs, UK; diluted 1 : 1000), $p21^{waf1/cip1}$ (Santa Cruz Biotechnology, USA; diluted 1 : 250), p53 (Calbiochem, Germany; diluted 1 : 100), IGF-1R (R&D Systems, USA; diluted 1 : 250), ERBB-2 (Oncogene Science, USA; diluted 1 : 1000), and IGF-1 (R&D Systems, USA; diluted 1 : 250). A secondary antibody linked to anti-mouse (Amersham Biosciences, UK; diluted 1 : 1000) or anti-goat (Sigma, USA; diluted 1 : 3000) horseradish peroxidase was used. The signal was visualized by a Western Lightening Chemiluminescence Reagent Plus kit (Perkin Elmer, USA) on the VersaDoc Imaging System 4000 (Bio-Rad, USA). Signal intensities of the particular bands were compared by Quantity One software (Bio-Rad, USA). Tubulin content varied across samples and was not suitable as a loading control. Amido-black staining (Sigma, USA) was used instead [9].

Immunohistochemistry

Immunohistochemical analysis of ERBB-2, p53, p-JNK, and IGF-1R protein was performed on formalin-fixed, paraffin-embedded tissue of four randomly chosen patients suffering from DD in triplicate. Protein expression was analysed using mouse monoclonal antibodies for ERBB-2 (c-neu/Ab-3) (Calbiochem, USA), p53 (Ab-6) (Calbiochem, USA), and p-JNK (G-7) (Santa Cruz Biotechnology, USA). Expression of IGF-1R protein was analysed using goat monoclonal antibody (AF-305-NA) (R&D Systems, USA).

After deparaffinization in xylene, slides were rehydrated in ethanol and washed in phosphate-buffered saline (PBS) (3 × 3 min). Endogenous peroxidase activity was quenched by 15-min incubation in methanol with 3% hydrogen peroxide (Sigma Chemical Co, Germany). The Target retrieval procedure involved immersion of tissue sections on slides in DAKO® Target Retrieval Solution (DAKO Corporation, USA) and heating in a microwave oven (600 W, 3 × 5 min). Slides were then allowed to cool for 30 min at room temperature. This step was omitted for immunohistochemical detection of ERBB2 protein. In all cases, non-specific binding was blocked by applying DAKO® Protein Block Serum-Free (DAKO Corporation, USA) in a humidity chamber for 10 min at room temperature. Slides were blotted and the primary antibodies at concentrations 1 : 10 (for IGF-1R), 1 : 20 (for ERBB-2, p53), and 1 : 50 (for p-JNK) were applied overnight at 4 °C. Slides were then washed three times in PBS.

In immunohistochemical detection of ERBB2, p53, and p-JNK, secondary antibody (rabbit antibody to mouse immunoglobulins; DAKO Corporation, USA), diluted with PBS and normal human serum [40 μl of rabbit anti-(mouse IgG) Ab, 100 μl of normal human serum, and 860 μl of PBS] was applied for 1 h at room temperature. Finally, peroxidase/anti-peroxidase (DAKO Corporation, USA) conjugate diluted 1 : 100 in PBS was applied for 45 min at room temperature. DAKO EnVision™ + System, HRP (DAB) (DAKO Corporation, USA) was used for visualization of a positive reaction according to the manufacturer's instructions. In immunohistochemical detection of IGF-1R, the HRP–DAB goat cell and tissue staining kit (R&D Systems, USA) was used according to the manufacturer's instructions. The slides were counterstained with haematoxylin for 30 s, dehydrated, and mounted in Canada balsam. Each slide was evaluated in the entire area. Results were expressed as negative or positive staining.

Results

Diseased and their corresponding unaffected palmar fasciae tissues were lysed in either CHAPS or ASB-14-based buffers differing in the solubilization properties. ASB-14-based buffer proved to be more efficient in solubilizing proteins than CHAPS-based buffer (800 versus 473 valid protein spots). CHAPS produced higher quality gels with better resolution (Figure 1). We managed to detect 28 overexpressed proteins in the gels obtained by CHAPS, in comparison with 20 obtained by ASB-14 in diseased tissues (Figure 2). Only adenylate kinase isoenzyme 4 (AK3L1) was diminished in level in the diseased palmar fasciae (Table 1).

Based on the proteomic data obtained, we created a protein–protein interactions map (interactome), as described in the Materials and methods section, which depicts the cellular processes associated with DD progression (Figure 3). The proteins involved therein fall into four discrete functional and structural classes described as follows (Table 1).

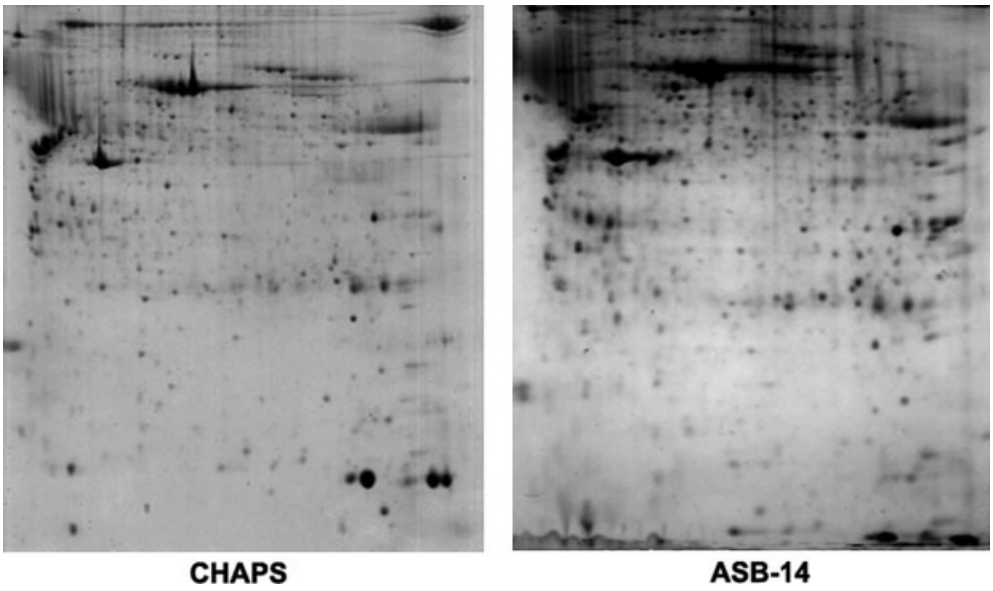

Figure 1. Typical 2-DE gels of diseased palmar fascia derived from Dupuytren's disease patients. Two common detergents, CHAPS and ASB-14, were used for sample preparation

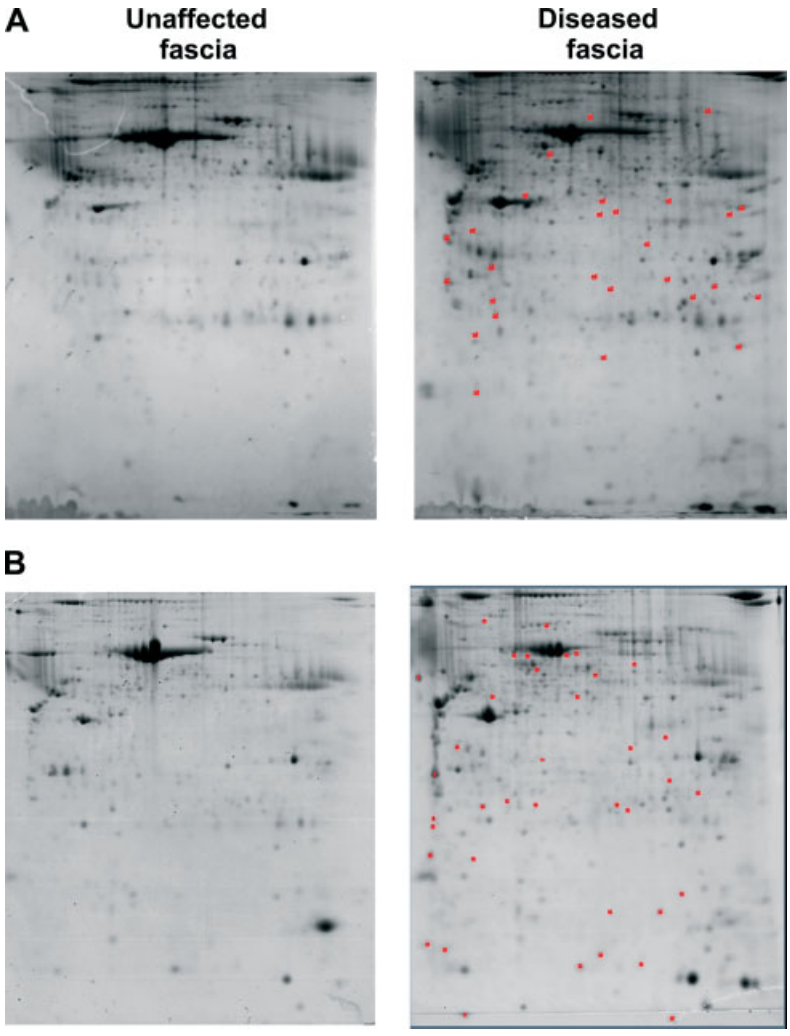

Figure 2. Representative 2-DE gels obtained from unaffected and patient-matched diseased palmar fasciae. Panels A and B represent the gels obtained by ASB-14- and CHAPS-based 2-DE buffers, respectively. The gels were stained by colloidal Coomassie blue and analysed by PDQuest software. Proteins that were differentially expressed (five-fold change) between unaffected and diseased samples in these respective gels for a given detergent are marked as red squares

Table 1. Differentially expressed proteins between diseased and unaffected patient-matched palmar fasciae obtained from patients suffering from Dupuytren's disease. In order to monitor abundant cellular changes which might account for the disease symptoms, only proteins with five-fold changes in all gels from diseased tissues relative to unaffected ones were identified. Overexpressed proteins are presented here

Protein name	Primary accession number (Uniprotkb/Swiss-prot)	Theoretical pI/MW	2-DE detergent		Protein score	Protein score (CI %)	Peptide count
			CHAPS	ASB-14			
Extra- and intra-cellular signalling proteins							
Collagen alpha-3(VI) chain (COL6A3)	P12111	6.4/34 5050.6	•	•	220	100	13
Microfibril-associated glycoprotein 4 (MFAP4)	P55083	5.4/28 972	•		184	100	10
Transforming growth factor-beta-induced protein ig-h3 (TGFBI)	Q15582	7.6/75 261.2	•	•	474	100	26
Rho GDP-dissociation inhibitor 1 (ARHGDIA)	P52565	5.0/23 118.7		•	193	100	10
Poly(rC)-binding protein 1 (PCBP1)	Q15365	6.7/37 987.1	•		169	100	7
Lung cancer oncogene 7 (RACK1)	Q5VLR4	8.5/38 378.2		•	294	100	16
Pigment epithelium-derived factor (SERPINF1)	P36955	5.9/46 484.4	•		321	100	16
Transitional endoplasmic reticulum ATPase (valosin-containing protein) (VCP)	P55072	5.1/89 818.9	•		353	100	28
Oxidative stress proteins							
Isocitrate dehydrogenase (NADP) cytoplasmic (IDH1)	O75874	6.5/46 914.6		•	303	100	21
Alpha-crystallin B chain (CRYAB)	P02511	6.7/20 146.4	•		276	100	13
Calreticulin (CALR)	P27797	4.3/48 282.9	•		514	100	22
Peroxiredoxin-1 (PRDX1)	Q06830	8.3/22 324.4		•	366	100	17
Oncogene DJ1 (PARK7)	Q99497	6.3/20 049.6		•	148	100	12
Heterogeneous nuclear ribo-nucleoprotein H3 (HNRPH3)	P31942	5.4/36 960.1	•	•	100	100	10
Heat-shock cognate 71 kD protein (HSPA8)	P11142	5.4/71 082.3		•	157	100	11
Heat-shock 70 kD protein 1 (HSPA1A)	P08107	5.5/70 294.1		•	261	100	12
Stress-induced-phosphoprotein 1 (STIP1)	P31948	6.4/63 226.6	•		350	100	25
Cytoskeleton proteins							
Cytokeratin-9 (KRT9)	P35527	5.2/62 320		•	59	95.5	11
Keratin 10 (KRT10)	Q8N175	5.1/59 019.7		•	148	100	15
Actin, cytoplasmic 2 (ACTG1)	P63261	5.3/42 107.9		•	151	100	15
Plastin 3 (PLS3)	Q5JRN9	5.5/70 904.3	•		460	100	27
T-complex protein 1 subunit beta (CCT2)	P78371	6.0/57 663.2	•		287	100	17
Vimentin (VIM)	P08670	5.2/49 680.1	•		475	100	21
Galectin-1 (LGALS1)	P09382	5.3/14 917.3	•		269	100	9
Transgelin (TAGLN)	Q01995	8.9/22 522.4	•		346	100	17
Tropomyosin 2 (beta) (TPM2)	Q5TCU3	4.6/32 908.6		•	158	100	14
Tropomyosin 4 (TPM4)	Q5U0D9	4.7/28 618.5	•		536	100	21
Tropomyosin alpha-4 chain (TPM4)	P67936	4.7/28 487.5		•	68	99.4	11
Myosin light polypeptide 3 (MYL3)	P08590	5.0/21 957.9	•		264	100	11
Myosin light polypeptide 6 (MYL6)	P60660	4.5/17 121.2	•		252	100	8
Gelsolin (GSN)	P06396	5.9/86 043.3	•		411	100	24
Cellular metabolism proteins							
Triosephosphate isomerase (TPI1)	Q6FHP9	6.4/26 937.8	•		374	100	15
Glyceraldehyde-3-phosphate dehydrogenase (GAPDH)	P04406	8.6/36 070.4	•	•	339	100	11
Pyruvate kinase isoenzymes M1/M2 (PKM2)	P14618	7.9/58 339.2		•	100	90	12
L-lactate dehydrogenase B chain (LDHB)	P07195	5.7/36 769.2	•		266	100	13
Glycyl-tRNA synthetase (GARS)	P41250	6.6/83 827.9		•	88	99.9	17
Phosphoglycerate kinase 1 (PGK1)	P00558	8.3/44 854.2		•	361	100	18

Table 1. Continued

Protein name	Primary accession number (Uniprotkb/Swiss-prot)	Theoretical pI/MW	2-DE detergent		Protein score	Protein score (CI %)	Peptide count
			CHAPS	ASB-14			
Adenylate kinase isoenzyme 4, mitochondrial (AK3L1)	P27144	8.5/25 268	•		324	100	27
Fatty acid-binding protein, adipocyte (FABP4)	P15090	6.8/14 692.5	•		253	100	8
Fatty acid-binding protein, epidermal (FABP5)	Q01469	6.8/15 365.6	•		282	100	12
Galactokinase (GALK1)	P51570	6.0/42 701.7		•	83	99.9	12
Histidine triad nucleotide-binding protein 1 (HINT1)	P49773	6.5/13 776.1	•		87	99.9	5
Ubiquitin B (UBB)	Q5U5U6	6.9/25 802.9	•		325	100	6
Nicotinamide N-methyltransferase (NNMT)	P40261	5.6/30 011.2	•		232	100	7

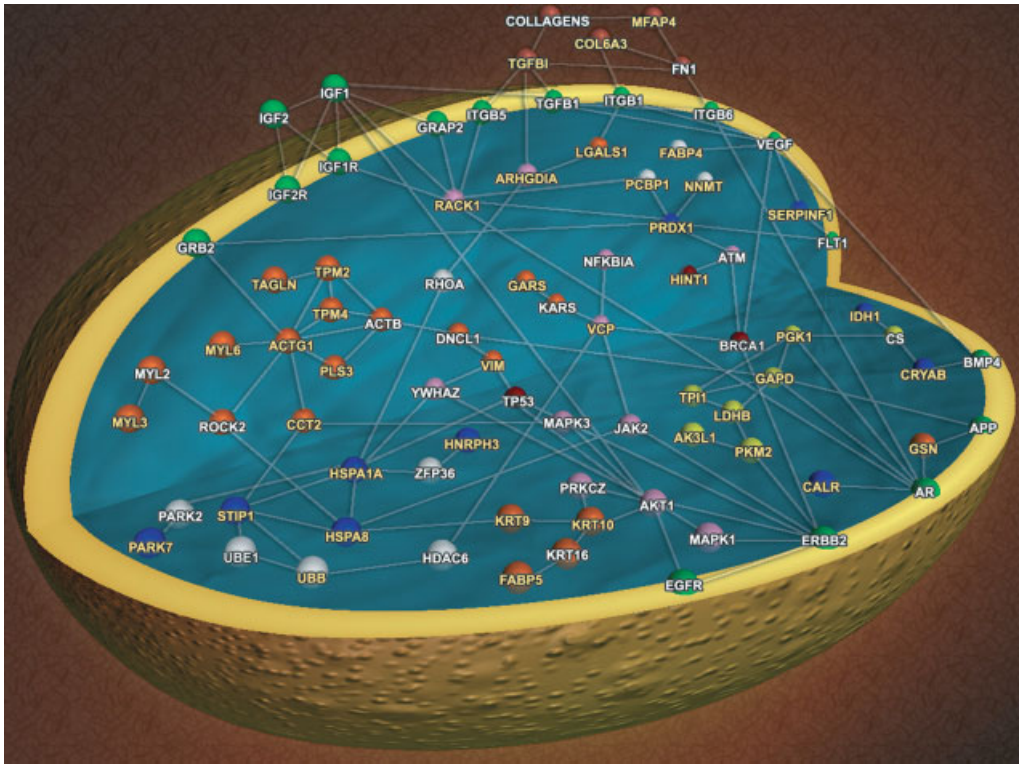

Figure 3. Interactome map of the proteins involved in the pathogenesis of DD. Several partial interactomes obtained from HiMAP and STRING were combined to obtain a single graphical representation. Proteins are depicted as beads marked with their respective gene names. Names of the proteins obtained by our proteomics analyses are highlighted in yellow. The beads are coloured in accordance with the protein function: extracellular matrix proteins — brown; receptors and ligands — green; cell signalling molecules — purple; tumour-suppressors — magenta; oxidative stress — blue; cytoskeleton components — orange; glycolysis — yellow; other — white. Gene names added to the original set and used to complete the interactome are listed in the Supporting information, Supplementary Table 1

The levels of two extracellular matrix (ECM) proteins, collagen alpha-3(VI) chain (COL6A3), and microfibril-associated glycoprotein 4 (MFAP4), were elevated in affected tissues. COL6A3 is often co-expressed with collagen type III, which is a histological marker in DD known to inhibit apoptosis during fibrosis [10] and facilitate differentiation of cardiac fibroblasts into myofibroblasts [11]. We also found transforming growth factor beta-induced protein ig-h3 (TGFBI), Rho GDP-dissociation inhibitor 1 (ARHGDIA), and poly(rC)-binding protein 1 (PCBP1) to be overexpressed in diseased tissues, which supports the previously established role of TGF-β signalling in DD.

The interactome map (Figure 3) suggested a role for other growth factors and their respective receptors in DD, eg v-erb-b2 erythroblastic leukaemia viral oncogene homologue 2 (ERBB-2) receptor and insulin-like growth factor receptor 1 (IGF-1R). Western blot analysis and immunohistochemistry results confirmed increased expression of ERBB-2 and IGF-1R receptors in diseased tissues (Figures 4 and 5). In

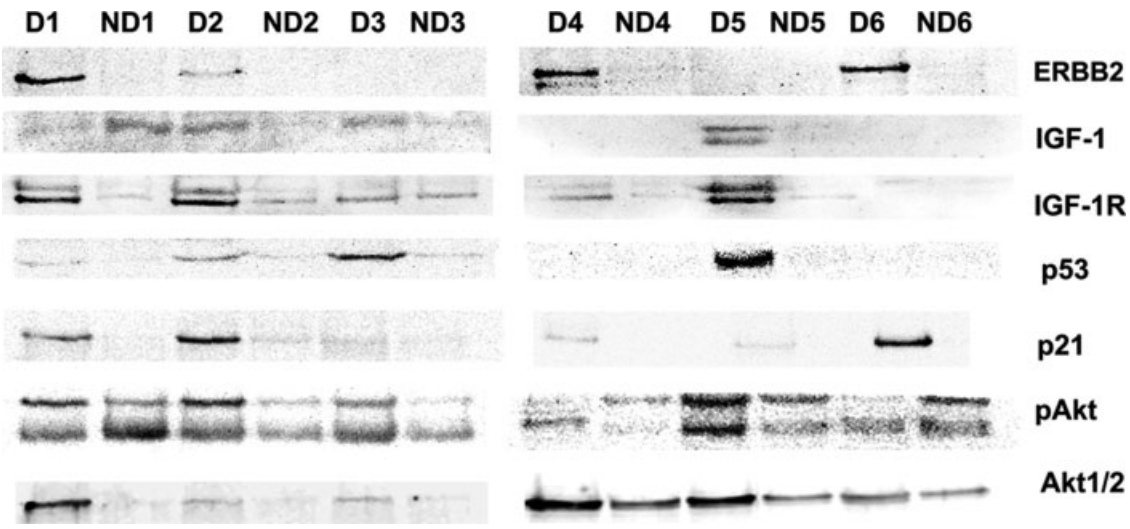

Figure 4. Representative western blots obtained from diseased (D) and patient-matched unaffected (ND) palmar fasciae. Tubulin content varied across the samples and therefore amido-black staining (Sigma, USA) was used as a loading control

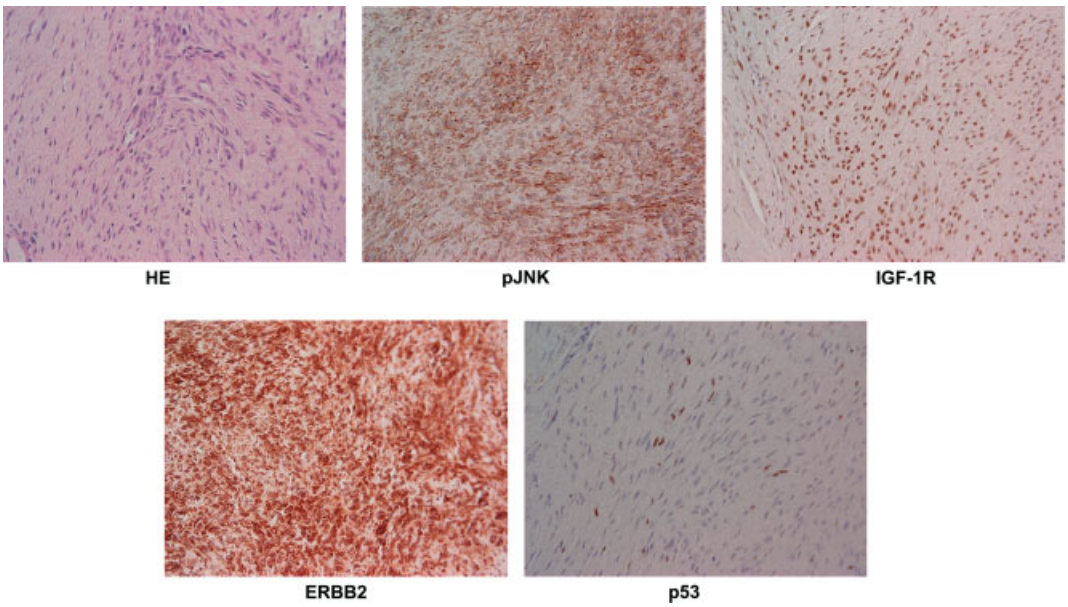

Figure 5. p-JNK, IGF-1R, ERBB-2, and p53 protein expression in diseased palmar fasciae of patients suffering from DD. Immunohistochemical staining patterns of p-JNK, IGF-1R, ERBB-2, and p53 proteins were obtained by using original magnification $\times$ 400. The control slides were counterstained with haematoxylin and eosin (HE)

addition, the interactome indicated the involvement of the phosphatidylinositol-3 kinase (PI-3K)/Akt signalling pathway in DD progression. This possibility was further corroborated by western blot revealing up-regulated levels of total Akt (Akt1/2/3) and phosphorylated Akt at serine site 473 (pAkt), as well as of two known Akt targets, p53 and $p21^{waf1/cip1}$, in diseased palmar fasciae. Interestingly, the immunohistochemistry results revealed moderately increased levels of the p53 protein as well as high levels of another protein known to be activated by phosphorylation, namely the pJNK protein, in diseased palmar fasciae (Figure 5). Furthermore, proteomic analysis revealed elevated levels of lung cancer oncogene 7 (RACK1), an important mediator of IGF-1-induced Akt phosphorylation [12], and valosin-containing protein (VCP), a down-stream target of the (PI-3K)/Akt cascade required for cell survival [13].

The role of ROS in DD pathogenesis has already been suggested [14,15]. We detected increased levels of isocytrate dehydrogenase 1 (IDH1), directly involved in the maintenance of the cellular redox state [16]; alpha-crystalin B chain (CRYAB), important in the cellular adaptation to environmental stress [17]; and calreticulin (CALR), an endoplasmic reticulum stress protein with the ability to block oxidative stress. Besides, identified anti-oxidant proteins peroxiredoxin-1 (PRDX1) and oncogene DJ1 (PARK7) are known to be involved in apoptosis inhibition, fibrosis development, and tumour cell growth as well.

Finally, we identified heterogeneous nuclear ribonucleoprotein H3 (HNRPH3), indispensable for the early heat-shock-induced splicing arrest [18].

Several heat-shock proteins (HSPs) were also detected in this study. Heat-shock cognate 71 kD protein (HSPA8) and heat-shock 70 kD protein 1 (HSPA1A) are, for example, produced by the cells in response to oxidative stress. Finally, we identified stress-induced phosphoprotein 1 (STIP1), which serves as an adaptor molecule for HSPA8.

We observed cytoskeletal changes not previously described in DD. Some of the identified proteins participate in cellular reshaping and cell growth control, eg cytoplasmic actin 2 (ACTG1) and plastin 3 (PLS3). Furthermore, T-complex protein 1 subunit beta (CCT2) is responsible for actin and tubulin folding during cell proliferation, and vimentin (VIM) provides structural stability. In addition, we detected elevated levels of galectin 1 (LGALS1), suggested to drive fibroblast differentiation into myogenic cells [19], and of the smooth muscle cell (SMC) marker transgelin (TAGLN), found in both fibroblasts and smooth muscles. Several proteins whose levels were increased in diseased tissues, including tropomyosin 2 (TPM2), tropomyosin alpha-4 chain (TPM4), and myosin light polypeptides 3 and 6 (MYL3 and MYL6), might actively participate in generation of the contractile force by myofibroblasts, which gives rise to the permanent finger contracture. Finally, increased levels of gelsolin (GSN) pointed to the deregulation of apoptosis in DD, as this physiological regulator of the actin cytoskeleton was found to prevent apoptosis in senescent human diploid fibroblasts.

Previous studies reported on alterations in the metabolic activity of the DD tissues [20]. We identified the following glycolytic proteins: triosephosphate isomerase (TPI1), glyceraldehyde-3-phosphate dehydrogenase (GAPDH), pyruvate kinase isoenzymes M1/M2 (PKM2), and L-lactate dehydrogenase B chain (LDHB). The remaining metabolic enzymes with raised levels were glycyl-tRNA synthetase (GARS) and phosphoglycerate kinase 1 (PGK1).

Discussion

Although Dupuytren's disease was first reported more than 175 years ago, the root causes still remain unknown. Recently, oxidative stress has been proposed to be a mechanism driving the onset of this disease [21,22]. Several proteins with increased levels in the affected palmar fasciae identified in this study play a role in the cellular protection against oxidative stress, eg CRYAB and PRDX1, known as negative regulators of apoptosis during the cellular response to oxidative stress. CRYAB is believed to exert its anti-apoptotic action through interaction with p53 protein, which prevents p53 translocation from the cytoplasm to mitochondria after oxidative stress [23]. The elevated p53 level in DD confirmed by western blotting could thus result from an oxidative insult. Additionally, the up-regulation of two HSP70 family members, HSPA8 and HSPA1A, highlights the role of oxidative stress in DD. The HSP70s are known to rescue cells from apoptotic/necrotic death after oxidative stress [24,25].

DD is similar to other fibroses and is defined as the pathological process encompassing the wound healing response [1], which elicits an overproduction of ECM via growth factor stimulation. The results of the present study similarly suggest that aberrant growth factor secretion represents a crucial step in the development of DD symptoms. For example, several of the proteins identified, including TGFBI, PCBP-1, and ARHGDIA, belong to the TGF-β signalling pathway. TGF-β was previously found to be the most abundant growth factor in DD [26]. The major roles of TGF-β in the differentiation of fibroblasts into myofibroblasts are activation of platelets and increased production of ECM [26]. Indeed, we identified two ECM proteins, MFAP4 and COL6A3, to be overexpressed in the affected tissues. COL6A3 partially constitutes collagen type VI. TGF-β can either up- or down-regulate the mRNA levels of COL6A3, and could therefore augment the specific role of collagen type VI in DD [27, 28]. Moreover, COL6A3 might play a role in cardiac myofibroblast differentiation [11].

The proposed interactome map revealed the receptors IGF-1R and ERBB2 as new molecular candidates that might be involved in autocrine regulation of cellular proliferation in DD. This result was confirmed by immunohistochemistry as well. ERBB-2 can assume a proliferative role through activation of the PI-3K/Akt pathway [29], while activation of IGF-1R through its specific ligand IGF-1 causes activation of the Ras/Raf/mitogen-activated protein kinase (MAPK) cascade and the PI-3K/Akt pathway with diverse physiological outcomes, including proliferation, differentiation, and inhibition of apoptosis [30]. RACK1, an important mediator of the IGF-1-induced Akt phosphorylation [31] that was detected in diseased fascia, might figure as a positive mediator of the ECM production. Further on, we detected up-regulated levels of total Akt (Akt1/2/3) in diseased tissues and phosphorylated Akt (pAkt) both in diseased and in patient-matched unaffected fascia, which again brings attention to the role of Akt in DD progression. Once activated, Akt promotes cell survival by phosphorylating substrates that decrease the activity of pro-apoptotic or increase the activity of anti-apoptotic proteins. Its activation was found to be a critical component of anti-apoptotic signalling in fibroblasts [32]. Our proteomic study is in line with western blotting findings unveiling overexpression of down-stream targets of PI-3K/Akt signalling, including VCP, $p21^{waf1/cip1}$, and p53 in diseased tissues. However, our results confirming increased levels of p53 protein in diseased fascia both by western blotting and by immunohistochemistry, contrast those of

Muller *et al*, who did not detect this protein in DD tissues by immunohistochemistry [33]. Increased expression of the $p21^{waf1/cip1}$ protein might account for the pronounced proliferation of fibroblasts in DD tissues upon stimulation with growth factors, as Quasnichka *et al* found that vascular smooth muscle cells were stimulated by growth factors to proliferate via regulation of the $p21^{waf1/cip1}$ gene [34]. Finally, the up-regulation of PARK7 augments the possibility of the involvement of PI-3K/Akt signalling in DD progression, as it suppresses the function of PTEN, a tumour suppressor that inhibits Akt-mediated cell survival [35].

This signalling pathway is also potentially responsible for the dynamic re-organization of the actin cytoskeleton known to occur during DD progression. In addition to ACTG1, several other proteins that are known to contribute to the formation of the phenotype characteristic for DD, eg PLS3, CCT2, VIM, and GSN, were identified in our study. We also found two cytoskeleton proteins novel to DD that might underlie the aberrant discontinuous proliferation resulting in myofibroblast differentiation: LGALS1, a regulator of fibroblast differentiation into myogenic cells [19], and TAGLN, an SMC differentiation marker induced upon TGF-β stimulation [36]. They could serve as novel differentiation markers for DD. The expression of several protein constituents of the smooth muscle contraction revealed in our study (eg TPM2, TPM4, MYL3, and MYL6) substantiates the formation of contractile force and permanent contracture present in the final stage of the disease.

In conclusion, combining proteomics data with bioinformatics processing provided a comprehensive insight into the molecular processes underlying DD progression. Our results turn the spotlight on the role of oxidative stress, autocrine deregulation, and activation of Akt in DD progression. Additional studies on a larger patient population are already under way in our laboratory.

Acknowledgements

We would like to thank Stipe Splivalo for assistance with the graphical preparation of the interactome map, and Professor Peter Stambrook, PhD, for useful suggestions during the preparation of the manuscript. This paper was financially supported by the Croatian Ministry of Science, Education and Sport's grants entitled 'Molecular characteristic of myofibroblasts derived from Dupuytren's contracture' (098-0982464-2393), JEZGRE-TEST 'Centre for integrative genomics, molecular diagnostic, cell and gene therapy' (14M09800), and the National Employment and Development Agency grant 'Development of a drug intended for treating the Dupuytren's disease patients' (14V09809). Parts of the proteomics study were performed at and financed by the Functional Genomics Center Zürich.

Supporting information

Supporting information may be found in the online version of this article.

References

1. Cordova A, Tripoli M, Corradino B, Napoli P, Moschella F. Dupuytren's contracture: an update of biomolecular aspects and therapeutic perspectives. *J Hand Surg (Br)* 2005;**30:**557–562.
2. Hart MG, Hooper G. Clinical associations of Dupuytren's disease. *Postgrad Med J* 2005;**81:**425–428.
3. Murrell GA, Francis MJ, Bromley L. Modulation of fibroblast proliferation by oxygen free radicals. *Biochem J* 1990;**265:**659–665.
4. Kraljevic S, Sedic M, Scott M, Gehrig P, Schlapbach R, Pavelic K. Casting light on molecular events underlying anti-cancer drug treatment: what can be seen from the proteomics point of view? *Cancer Treat Rev* 2006;**32:**619–629.
5. Zhang D, Tai LK, Wong LL, Chiu LL, Sethi SK, Koay ES. Proteomic study reveals that proteins involved in metabolic and detoxification pathways are highly expressed in HER-2/neu-positive breast cancer. *Mol Cell Proteomics* 2005;**4:**1686–1696.
6. Perkins DN, Pappin DJ, Creasy DM, Cottrell JS. Probability-based protein identification by searching sequence databases using mass spectrometry data. *Electrophoresis* 1999;**20:**3551–3567.
7. Rhodes DR, Tomlins SA, Varambally S, Mahavisno V, Barrette T, Kalyana-Sundaram S, *et al*. Probabilistic model of the human protein–protein interaction network. *Nature Biotechnol* 2005;**23:**951–959.
8. von Mering C, Jensen LJ, Kuhn M, Chaffron S, Doerks T, Kruger B, *et al*. STRING 7 — recent developments in the integration and prediction of protein interactions. *Nucleic Acids Res* 2007;**35:**D358–D362.
9. Gire V, Roux P, Wynford-Thomas D, Brondello J, Dulic V. DNA damage checkpoint kinase Chk2 triggers replicative senescence. *EMBO J* 2004;**23:**2554–2563.
10. Ruhl M, Sahin E, Johannsen M, Somasundaram R, Manski D, Riecken EO, *et al*. Soluble collagen VI drives serum-starved fibroblasts through S phase and prevents apoptosis via down-regulation of bax. *J Biol Chem* 1999;**274:**34361–34368.
11. Naugle JE, Olson ER, Zhang X, Mase SE, Pilati CF, Maron MB, *et al*. Type VI collagen induces cardiac myofibroblast differentiation: implications for postinfarction remodeling. *Am J Physiol Heart Circ Physiol* 2006;**290:**H323–H330.
12. Kiely PA, Sant A, O'Connor R. RACK1 is an insulin-like growth factor 1 (IGF-1) receptor-interacting protein that can regulate IGF-1-mediated Akt activation and protection from cell death. *J Biol Chem* 2002;**277:**22581–22589.
13. Vandermoere F, El Yazidi-Belkoura I, Slomianny C, Demont Y, Bidaux G, Adriaenssens E, *et al*. The valosin-containing protein (VCP) is a target of Akt signaling required for cell survival. *J Biol Chem* 2006;**281:**14307–14313.
14. Duthie RB, Francis MJ. Free radicals and Dupuytren's contracture. *J Bone Jt Surg Br* 1988;**70:**689–691.
15. Murrell GA, Francis MJ, Bromley L. Free radicals and Dupuytren's contracture. *Br Med J (Clin Res Ed)* 1987;**295:**1373–1375.
16. Lee SM, Koh HJ, Park DC, Song BJ, Huh TL, Park JW. Cytosolic NADP(+)-dependent isocitrate dehydrogenase status modulates oxidative damage to cells. *Free Radic Biol Med* 2002;**32:**1185–1196.
17. Neufer PD, Benjamin IJ. Differential expression of alpha-B-crystallin and Hsp27 in skeletal muscle during continuous contractile activity — relationship to myogenic regulatory factors. *J Biol Chem* 1996;**271:**24089–24095.
18. Nakamura M, Yamada M, Ohsawa T, Morisawa H, Nishine T, Nishimura O, *et al*. Phosphoproteomic profiling of human SH-SY5Y neuroblastoma cells during response to 6-hydroxydopamine-induced oxidative stress. *Biochim Biophys Acta* 2006;**1763:**977–989.
19. Goldring K, Jones GE, Thiagarajah R, Watt DJ. The effect of galectin-1 on the differentiation of fibroblasts and myoblasts *in vitro*. *J Cell Sci* 2002;**115:**355–366.
20. Delbruck A, Reimers E, Schonborn I. A comparative study of the activity of lysosomal and main metabolic pathway enzymes in tissue biopsies and cultured fibroblasts from Dupuytren's disease

and palmar fascia. On the pathobiochemistry of connective tissue proliferation, I. *J Clin Chem Clin Biochem* 1981;**19:**931–941.
21. Bayat A, Walter J, Lambe H, Watson JS, Stanley JK, Marino M, *et al*. Identification of a novel mitochondrial mutation in Dupuytren's disease using multiplex DHPLC. *Plast Reconstr Surg* 2005;**115:**134–141.
22. Lu CY, Lee HC, Fahn HJ, Wei YH. Oxidative damage elicited by imbalance of free radical scavenging enzymes is associated with large-scale mtDNA deletions in aging human skin. *Mutat Res* 1999;**423:**11–21.
23. Liu S, Li J, Tao Y, Xiao X. Small heat shock protein alphaB-crystallin binds to p53 to sequester its translocation to mitochondria during hydrogen peroxide-induced apoptosis. *Biochem Biophys Res Commun* 2007;**354:**109–114.
24. Klein SD, Brune B. Heat-shock protein 70 attenuates nitric oxide-induced apoptosis in RAW macrophages by preventing cytochrome c release. *Biochem J* 2002;**362:**635–641.
25. Ravagnan L, Gurbuxani S, Susin SA, Maisse C, Daugas E, Zamzami N, *et al*. Heat-shock protein 70 antagonizes apoptosis-inducing factor. *Nature Cell Biol* 2001;**3:**839–843.
26. Al-Qattan MM. Factors in the pathogenesis of Dupuytren's contracture. *J Hand Surg (Am)* 2006;**31A:**1527–1534.
27. Lamande SR, Morgelin M, Adams NE, Selan C, Allen JM. The C5 domain of the collagen VI alpha3(VI) chain is critical for extracellular microfibril formation and is present in the extracellular matrix of cultured cells. *J Biol Chem* 2006;**281:**16607–16614.
28. Lamande SR, Sigalas E, Pan TC, Chu ML, Dziadek M, Timpl R, *et al*. The role of the alpha3(VI) chain in collagen VI assembly. Expression of an alpha3(VI) chain lacking N-terminal modules N10–N7 restores collagen VI assembly, secretion, and matrix deposition in an alpha3(VI)-deficient cell line. *J Biol Chem* 1998;**273:**7423–7430.
29. Casalini P, Iorio MV, Galmozzi E, Menard S. Role of HER receptors family in development and differentiation. *J Cell Physiol* 2004;**200:**343–350.
30. Vincent AM, Feldman EL. Control of cell survival by IGF signaling pathways. *Growth Horm IGF Res* 2002;**12:**193–197.
31. Hermanto U, Zong CS, Li WQ, Wang LW. RACK1, an insulin-like growth factor I (IGF-I) receptor-interacting protein, modulates IGF-I-dependent integrin signaling and promotes cell spreading and contact extracellular matrix. *Mol Cell Biol* 2002;**22:**2345–2365.
32. Kulik G, Klippel A, Weber MJ. Antiapoptotic signalling by the insulin-like growth factor I receptor, phosphatidylinositol 3-kinase, and Akt. *Mol Cell Biol* 1997;**17:**1595–1606.
33. Muller E, Castagnaro M, Yandel DW, Wolfe HJ, Alman BA. Molecular genetic and immunohistochemical analysis of the tumor suppressor genes Rb and P53 in palmar and aggressive fibromatosis. *Diagn Mol Pathol* 1996;**5:**194–200.
34. Quasnichka H, Slater SC, Beeching CA, Boehm M, Sala-Newby GB, George SJ. Regulation of smooth muscle cell proliferation by beta-catenin/T-cell factor signaling involves modulation of cyclin D1 and p21 expression. *Circ Res* 2006;**99:**1329–1337.
35. Kim RH, Peters M, Jang Y, Shi W, Pintilie M, Fletcher GC, *et al*. DJ-1, a novel regulator of the tumor suppressor PTEN. *Cancer Cell* 2005;**7:**263–273.
36. Kawai-Kowase K, Sato H, Oyama Y, Kanai H, Sato M, Doi H, *et al*. Basic fibroblast growth factor antagonizes transforming growth factor-beta1-induced smooth muscle gene expression through extracellular signal-regulated kinase 1/2 signaling pathway activation. *Arterioscler Thromb Vasc Biol* 2004;**24:**1384–1390.